Domain–Domain Communication in Aminoacyl-tRNA Synthetases

REBECCA W. ALEXANDER* AND PAUL SCHIMMEL†

*Department of Chemistry
Wake Forest University
Winston-Salem, North Carolina 27109
†The Skaggs Institute for Chemical Biology
The Scripps Research Institute
La Jolla, California 92037

Aminoacyl-tRNA synthetases are modular proteins, with domains that have distinct roles in the aminoacylation reaction. The catalytic core is responsible for aminoacyl adenylate formation and transfer of the amino acid to the 3′ end of the bound transfer RNA (tRNA). Appended and inserted domains contact portions of the tRNA outside the acceptor site and contribute to the efficiency and specificity of aminoacylation. Some aminoacyl-tRNA synthetases also have distinct editing activities that are localized to unique domains. Efficient aminoacylation and editing require communication between RNA-binding and catalytic domains, and can be considered as a signal transduction system. Here, evidence for domain–domain communication in aminoacyl-tRNA synthetases is summarized, together with insights from structural analysis. © 2001 Academic Press.

Progress in Nucleic Acid Research and Molecular Biology, Vol. 69

0079-6603/01 $35.00

I. Function and Domain Organization of AARSs

Aminoacyl-tRNA synthetases (AARSs) catalyze attachment of amino acids to cognate tRNAs, thereby establishing the rules of the genetic code (*1*). The AARS-catalyzed aminoacylation reaction occurs by a two-step mechanism. In the first step, enzyme-bound amino acid (AA) is converted to an activated aminoacyl adenylate (AA-AMP) by condensation with ATP. The second step is a thermodynamically favored transesterification of the amino acid to the 3′-OH of the cognate tRNA's terminal adenosine.

$$E + AA + ATP \rightleftharpoons E \cdot (AA\text{-}AMP) + PP_i$$

$$E \cdot (AA\text{-}AMP) + tRNA \rightleftharpoons AA\text{-}tRNA + E + AMP$$

For most systems the first step is independent of tRNA binding. GlnRS, GluRS, and ArgRS are the exceptional cases and require the presence of cognate tRNA for adenylate formation (2). (Throughout this article, individual AARSs are abbreviated according to the three-letter code of their corresponding amino acid.)

Because of their central role in translation, AARSs are thought to be among the earliest proteins to emerge from an RNA world (*3–5*). This family of isofunctional enzymes can be partitioned into two classes based on sequence and structural similarities of their catalytic domains (*6–9*). Class I AARSs have active sites built around a Rossmann nucleotide binding fold [first identified in dehydrogenases (*10*)]. Enzymes in class I contain (in their catalytic cores) an 11–amino acid signature sequence ending in HIGH (*6, 7*) and the pentapeptide KMSKS (*11*). The conserved residues stabilize the aminoacyl adenylate as it is formed in the active site. Class II AARSs have catalytic domains built around a seven-stranded antiparallel β-sheet bundle with three α-helices (*9, 12*). Enzymes in class II lack the class I HIGH and KMSKS sequences, instead, they have highly degenerate motifs 1, 2, and 3 that form a helix–loop–strand, strand–loop–strand, and strand–helix structure, respectively (*8*). Further structural and sequence similarities allow classification into subgroups (Table I). With a single exception the class distinctions have been conserved among all known AARSs (*13*).

In addition to these class-defining catalytic domains, most AARSs have nonconserved domains either appended to their N or C termini or inserted into the catalytic cores. These idosyncratic domains typically contact the cognate tRNA, providing binding energy and increasing specificity through interactions with recognition elements. The class-defining catalytic domains are thought to be the early aminoacylation enzymes, perhaps binding minimal RNA substrates such as minihelices and microhelices which are aminoacylated by many extant AARSs (Fig. 1). As substrate recognition became an increasing challenge, it was imagined that appended domains are recruited to bind identity elements outside the

TABLE I
DISTINCTIONS BETWEEN THE TWO CLASSES OF AMINOACRYL-tRNA SYNTHETASES

	Class I	Class II
Conserved sequence motifs	KMSKS, HIGH	Motif 1: ... P ... Motif 2: ... FRxE ... Motif 3: ... $(Gx)_3ER$
Conserved catalytic domain structure	Rossmann nucleotide binding fold (parallel β-sheet)	Antiparallel β-sheet
Site of A76 aminoacylation	2′-OH	3′-OH[a]
tRNA binding		
Acceptor stem	Minor groove side	Major groove side
Variable loop	Faces solvent	Faces protein

	Class Ia	Class Ib	Class IIa	Class IIb	Class IIc
Subclasses[b]	MetRSα_2		SerRSα_2		
	LeuRSα	GlnRSα	HisRSα_2	AspRSα_2	PheRS$\alpha_2\beta_2$
	IleRSα	GluRSα	GlyRSα_2	AsnRSα_2	AlaRSα_4
	ValRSα	TyrRSα_2	ProRSα_2	LysRSα_2	GlyRS$\alpha_2\beta_2$
	CysRSα	ThrRSα_2	ThrRSα_2		
	ArgRSα				

[a]Except for $tRNA^{Phe}$.
[b]The subunit composition (α, α_2, α_4, or $\alpha_2\beta_2$) is shown for the *E. coli* enzymes.
Adapted from Refs. *132* and *133*.

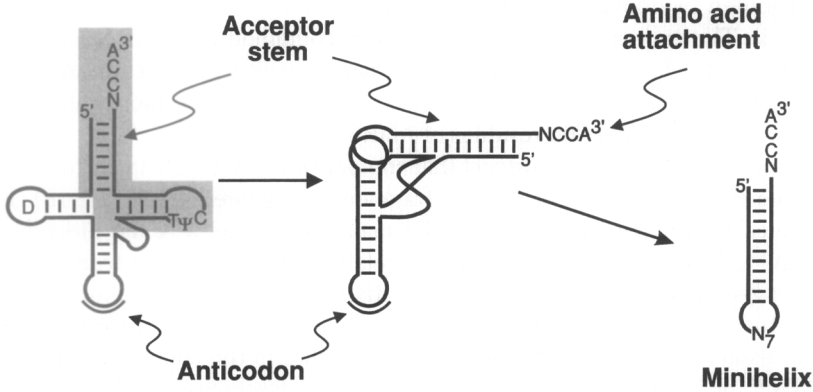

FIG. 1. The two-domain organization of tRNA. The cloverleaf structure of tRNA (left) folds in three dimensions into an L-shaped molecule (right). Many AARSs aminoacylate small RNA mimics of the tRNA acceptor arm (such as the minihelix).

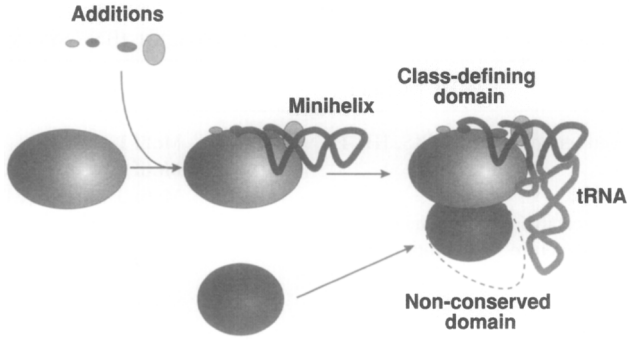

FIG. 2. The domain organization of AARSs. The class-defining catalytic core is thought to be the primordial aminoacylating enzyme, with other protein domains added to increase efficiency and specificity of aminoacylation. Likewise, the minihelix arm of tRNA is a minimal RNA substrate for many AARSs. Adapted from Ref. *129*.

amino acid acceptor 3′ terminus or to perform other functions such as editing (Fig. 2) (*14*, *15*).

II. Domain Functions Are Separable

As a framework for developing the concept of functional domains of AARSs, the class II alanyl-tRNA synthetase (AlaRS) can be considered. AlaRS is the largest *E. coli* AARS, active *in vivo* as a tetramer of 875-aa monomers (*16*). Sequential C-terminal deletions showed that the functions of AlaRS are contributed by domains organized in a linear fashion along the sequence (*17*) (Fig. 3). The canonical class II active site is contained in the N-terminal 242 residues. This first segment, however, is not in itself sufficient for any AlaRS function.Indeed, activation of alanine (the first step of the aminoacylation reaction) requires the first 368 residues of AlaRS (*16*, *17*).

The minimal protein construct that compensates for an AlaRS chromosomal deficiency is the N-terminal 461-aa fragment, designated 461N (*17*, *18*). Biochemical studies determined that AlaRS makes no contact with the anticodon of $tRNA^{Ala}$, thus demonstrating an indirect relationship between the trinucleotides of the genetic code for alanine and the tRNA determinants for aminoacylation (*19*). Instead, a unique G3:U70 wobble base pair in the acceptor stem of AlaRS is necessary and sufficient for alanylation, whether in the context of full-length $tRNA^{Ala}$ or in small RNA mimics (minihelices, microhelices, and duplexes) of the acceptor stem (*20–23*). Chemical mutagenesis demonstrated that AlaRS recognizes the exocyclic 2-amino group of G3 that is presented in the minor groove of the $tRNA^{Ala}$ acceptor helix (*24*).

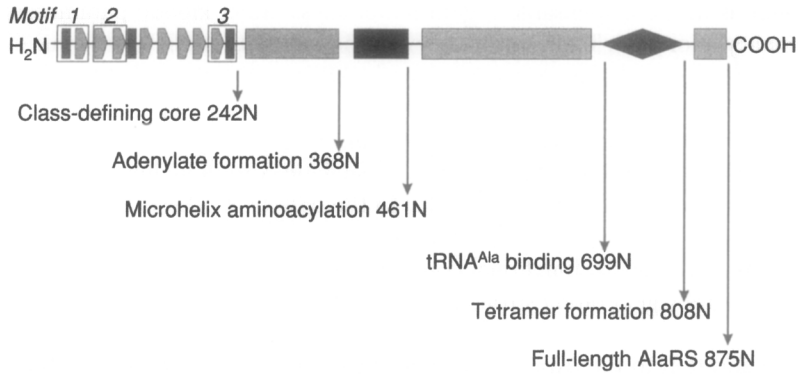

FIG. 3. Linear arrangement of AlaRS along the sequence, as predicted from sequence comparisons and functional analysis (*130*). Adapted from Ref. *131*.

Fragment 461N of AlaRS aminoacylated an RNA microhelix or duplex substrate with the same efficiency as that of the full-length enzyme (*25*). This sufficiency for microhelix aminoacylation suggested that residues necessary for specific G3:U70 recognition were contained within the 461N fragment. Indeed, crosslinking experiments localized the G3:U70-specific contacts to between Val 250 and Asp 461 (*26*). Mutational analysis and molecular modeling predicted a two-helix pair within this region that may function as a novel RNA-binding motif (*27*). The predicted two-helix recognition motif spans Leu 280 through Gly 320.

In contrast to the motif predicted to recognize the G3:U70 pair of $tRNA^{Ala}$, a separate domain contributes to nonspecific tRNA binding (*28*). Although fragment 461N can be considered a minimal enzyme (because it aminoacylates a microhelix efficiently), it aminoacylated full-length $tRNA^{Ala}$ with a catalytic efficiency (k_{cat}/K_M) that is decreased about 1000-fold compared to the full-length enzyme. This result showed that, although AlaRS makes no contact with the anticodon, functional tRNA contacts are missing in 461N. Indeed, binding interactions are recovered upon extension of AlaRS through the first 699 amino acids (*28*). Operationally, then, the region from His 462 to Gly 699 is a domain that contains additional RNA-binding determinants. As explained below, this domain also communicates with the active site that is located in the N-terminal domain (*29*).

A C-terminal domain is responsible for oligomerization of AlaRS. Truncation of the enzyme after Gly 699 resulted in a monomeric protein, while N-terminal fragments longer than 808 residues were tetrameric (*17*). This localized an oligomerization motif to the region between Gly 699 and Val 808. Although C-terminal truncation of AlaRS results in a functionally active monomer,

mutations in the dispensable region nonetheless affect kinetic parameters for aminoacylation (*30*). Thus, these early experiments with AlaRS gave some of the first evidence for domain organization of AARSs and showed that the domains could communicate.

The segregation of functions among the AlaRS domains is consistent with the notion that early AARSs consisted of catalytic core domains to which RNA binding domains were added (*14*, *15*). In the case of AlaRS, fragment 461N is the minimal protein able to efficiently aminoacylate a microhelix RNA. As other domains were added, functional communication was established between domains, thereby generating strong selective pressure to retain all domains of the protein.

In addition to the experiments with deletion proteins described above for AlaRS, mutagenesis of other AARSs has demonstrated that domain functions are in general separable for this family of enzymes. For example, deletion of 11 amino acids encompassing Trp 461, which is critical for anticodon recognition by *Escherichia coli* MetRS, dramatically reduced the efficiency of aminoacylation of $tRNA^{Met}$ (Table II) (*31*). Adenylate formation and microhelix aminoacylation were not affected by the deletion, thus demonstrating the integrity of the catalytic domain in the deleted protein. The converse analysis was also done. Arg 533 in the C-terminal domain of MetRS is proposed to orient (either directly or through allosteric means) the acceptor stem of $tRNA^{Met}$ for aminoacylation. An alanine substitution at this position (Arg533 → Ala) significantly decreased the catalytic efficiency of $tRNA^{Met}$ and $microhelix^{fMet}$ aminoacylation (principally by affecting acceptor-stem binding) but did not affect binding of an isolated anticodon stem–loop mimic of $tRNA^{fMet}$ (*32*).

TABLE II

KINETIC CONSTANTS FOR AMINOACYLATION OF $tRNA^{fMet}$ BY *E. coli* MetRS VARIANTS

MetRS	Relative adenylation (k_{cat}/K_M)	tRNA K_M (μM)	Aminoacylation k_{cat} (sec^{-1})	Relative aminoacylation (k_{cat}/K_M)	Microhelix aminoacylation	Ref.
Wild-type (547mer)	1	1.2 ± 0.2	3.2 ± 0.2	1		*134*
Trp461Phe	0.38	75 ± 15	4.3 ± 0.6	0.02		*134*
Trp461Ala				2.7×10^{-5}		*41*
Δ11(Tyr454–Ala464)	0.97			$<3 \times 10^{-4}$	As wild-type	*31*
Arg533Ala	0.65	50	0.8	2.6×10^{-2}	Greatly reduced	*32*
Arg395Gln	0.20	39 ± 9	$(4.7 \pm 0.6) \times 10^{-3}$	4×10^{-5}		*134*
Arg395Ala	0.43	113 ± 31	$(1.7 \pm 0.4) \times 10^{-2}$	6×10^{-5}		*134*

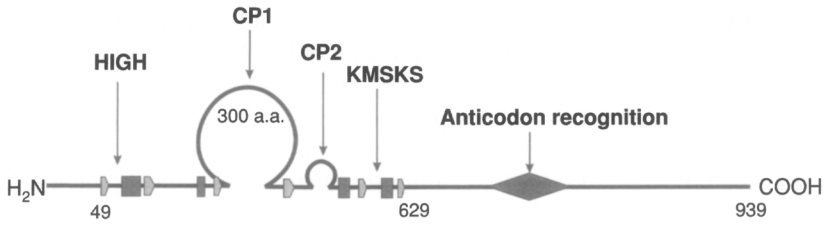

FIG. 4. Domain organization of *E. coli* IleRS. Connective polypeptides 1 and 2 (CP1 and CP2) interrupt the class I–defining Rossmann nucleotide binding fold, where β-strands are shown as arrows and helices as rectangles. Adapted from Ref. 33.

The adenylation and aminoacylation steps of the monomeric 939-aa *E. coli* IleRS can also be functionally separated. Lys 732 in the C-terminal half of the enzyme was proposed to play a role in IleRS similar to that of the anticodon-binding Trp 461 of MetRS. Substitution of Lys 732 resulted in variant enzymes severely defective in tRNA aminoacylation but fully functional for adenylate formation (33). Similar functional dissections have been done for the editing activity of IleRS that deacylates mischarged Val-$tRNA^{Ile}$. Thus, mutations that affect the editing function of IleRS do not affect adenylate synthesis or aminoacylation functions. For example, substitutions at Thr 252 and Asn 250 in the editing domain known as CP1 (Fig. 4) resulted in mutant enzymes that poorly hydrolyze misacylated Val-$tRNA^{Ile}$ but retain their capacity to form isoleucyl adenylate (34). Similarly, mutations at His 401 and Tyr 403 (also in CP1) produced IleRS variants with enhanced tRNA-dependent amino acid discrimination but unaltered activation and aminoacylation activities (35). Conversely, a mutation in the catalytic core of the enzyme (Gly56 → Ala) significantly reduced the valine versus isoleucine discrimination in the adenylate formation reaction without affecting deacylation of Val-$tRNA^{Ile}$ (36).

Thus, the demonstration by biochemistry and genetics of separable domains with specific functions for various AARSs established a rationale for domain–domain communication that ties these functions together.

III. Noncovalent Assembly of Aminoacylation Systems Demonstrating Capacity for Communication

Domain-domain communication in the most general sense can be seen by the noncovalent assembly of aminoacylation systems. In these examples, separate polypeptides associate at an interface to create an active structure. Undoubtedly, this association causes a structural change in each of the associating proteins.

Insertion of a stop signal and restart sequence into a plasmid-borne protein coding sequence results in the expression of isolated but cotranslationally produced polypeptides. Split proteins of *E. coli* MetRS have been constructed, and functional constructs have been produced, depending on the location of the split (37). For example, insertion of a stop–restart sequence after Arg 367 resulted in complementation *in vivo* of a chromosomal MetRS defect. This location for the split approximately divides the catalytic site from the anticodon-binding domain. Furthermore, both the N- and C-terminal fragments were expressed in quantities that could be purified, indicating that the polypeptides were stably produced. The fragments were reconstituted *in vitro* and the split MetRS aminoacylated $tRNA^{fMet}$ with an efficiency only minimally reduced relative to wild-type enzyme. Similar stop–start sequences were inserted at various locations in the region between the catalytic and anticodon-binding domains. MetRS constructs with splits after Arg 367, Ile 371, and Asn 374 complemented the chromosomal defect, while splits inserted after Ser 355, Tyr 358, and Lys 363 resulted in inactive proteins (37). These results demonstrated that the interface region of MetRS is particularly sensitive to structural perturbations that affect noncovalent packing interactions between the two functional domains.

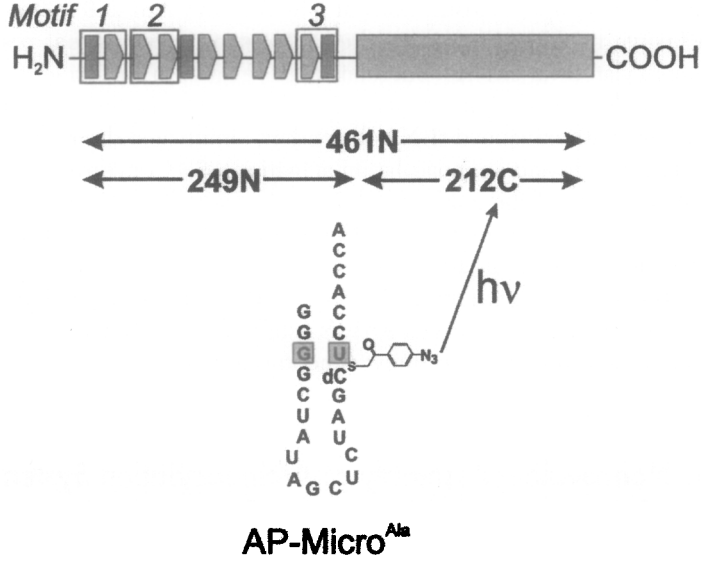

FIG. 5. Recognition of $tRNA^{Ala}$ localized to a specific region of AlaRS. An AlaRS split protein construct of the 461N fragment reconstituted $microhelix^{Ala}$ aminoacylation activity. An azidophenyl-derivatized (AP) microhelix containing the identity determinant G3:U70 was photocrosslinked to the 212C fragment (26).

The 461N fragment of AlaRS was also investigated using a split-protein construct (*26*). This functional core was expressed with a stop codon and restart sequence between His 249 and Val 250, to produce fragments 249N and 212C (Fig. 5). The fragments associated *in vitro* to aminoacylate the microhelix^{Ala} substrate in a manner that depended on the presence of the G3:U70 determinant. A photolabile derivative of microhelix^{Ala} crosslinked exclusively to the 212C fragment, and this crosslink was also G3:U70-dependent, indicating that residues Val 250 to Asp 461 of AlaRS are responsible for recognition of the tRNA^{Ala} acceptor stem. Indeed, it is within this domain of AlaRS that the putative two-helix RNA recognition motif was located by mutagenesis and modeling studies (*27*).

In the case of *E. coli* IleRS, more than 20 split-protein constructs have been created (*38, 39*). Most of these constructions generated active enzymes, including those involving three-piece assemblies (*39*). These results demonstrate the capacity of proteins like IleRS to combine as noncovalent pieces and induce active structures. This finding supports the idea that conformational flexiblity is inherent, and suggests the possibility that such flexibility can be incorporated into signaling mechanisms of native structures.

IV. Examples of Domain–Domain Communication Revealed by Functional Analysis of Aminoacylation Efficiency

In many cases, contributions to aminoacylation efficiency can be directly attributed to the amino acid transfer step (in isolation from tRNA binding and adenylate formation). Indeed, although some domains of AARSs contribute to tRNA binding (either nonspecific or sequence-dependent), these interactions are relatively weak, with dissociation constants at pH 7.5 on the order of 1 μM (*1, 40, 41*). This likely reflects the need for rapid release of aminoacylated tRNA for protein synthesis, and demonstrates the limited tRNA discrimination that can be achieved by binding alone. Numerous mutagenesis studies have established that substrate specificity is largely determined by kinetic rather than binding effects (*42*). Moreover, these kinetic effects result from domain–domain communication.

In particular, single-nucleotide substitutions in the *alaS* gene gave rise to two alleles, *alaS4* and *alaS5*. These alleles code for Gly 674 → Asp and Gly 677 → Asp substitutions, respectively. As might be expected from their locations near the AlaRS oligomerization domain, the products of these genes are monomeric (*30, 43*). Both mutant enzymes catalyze the synthesis of alanyl adenylate with essentially the same activity as that of wild-type enzyme. Thus, the catalytic site for adenylate formation is undisturbed by the mutations. In contrast, the rate

of aminoacylation of $tRNA^{Ala}$ is reduced (*30*). The primary defect is at the transition state for aminoacylation, with k_{cat} reduced 20-fold for the *alaS4* mutant protein and 10-fold for the *alaS5* mutant protein (relative to wild-type AlaRS). Therefore, although the mutations are in a dispensable region, this part communicates with the active center (*30*). To further prove this point, inactive AlaRS deletion constructs lacking essential portions of the catalytic site were shown to compensate for the aminoacylation defect in the *alaS5* protein (*43*). With the C-terminal (oligomerization) domain of the inactive deletion construct hybridized to the catalytic domain of the *alaS5* protein, activity was regenerated (Fig. 6). This demonstrates that the domain–domain communication function can come from isolated polypeptides. (Other examples of such "piecewise functional assembly" are presented below.)

At this writing, there is no crystal structure for AlaRS. It could be argued that the "communication" from the region involving Gly 674 and Gly 677 was, in fact, due to a direct contribution of this part of the structure to the mechanism of the aminoacyl transfer step (but not to adenylate formation). This possibility is unlikely, because the other experiments showed that k_{cat} for aminoacylation is essentially all determined by residues in fragment 461N (*25*).

In the case of AlaRS, where the key identity element (the G3:U70 base pair) is located in the acceptor stem, discrimination occurs both in the binding step and at the transition state. The relative contributions can be partitioned depending on pH (*23*). For example, at pH 7.5, $tRNA^{Ala}$ variants containing A3:U70, G3:U70, or U3:G70 substitutions were not aminoacylated by AlaRS (at either catalytic or substrate levels of enzyme). Furthermore, even high concentrations

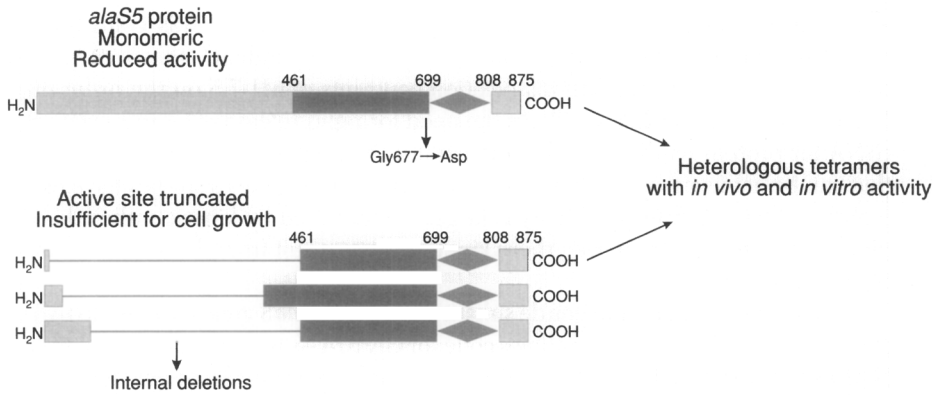

FIG. 6. Complementation of the *alaS5* chromosomal defect by AlaRS active site deletions. The *alaS5* protein is unable to sustain cell growth owing to a substitution in the AlaRS oligomerization domain. Constructs producing deletions in the catalytic core of AlaRS, such as those shown here, are themselves inactive, but are able to compensate for the *alaS5* defect and restore cell growth (*43*).

of the A3:U70 variant did not inhibit aminoacylation of wild-type $tRNA^{Ala}$, indicating that the variant was not bound specifically by AlaRS. Therefore, under physiological conditions, the lack of aminoacylation of A3:U70 $tRNA^{Ala}$ is at least in part due to an increase in the Michaelis constant (K_M). Interactions between AARSs and their cognate tRNAs are much stronger at lower pH values (*1*). This was verified in the case of $tRNA^{Ala}$:AlaRS complex formation (*23*). Binding of A3:U70 or G3:U70 $tRNA^{Ala}$ to AlaRS at pH 5.5 was only 3–5-fold weaker than binding of wild-type tRNA. However, although wild-type $tRNA^{Ala}$ was aminoacylated, alanylation of these tRNAs was not detected (*23*). Under these conditions, therefore, the effect on the catalytic rate constant (k_{cat}) dominates the discrimination between cognate and noncognate substrates. As explained above, k_{cat} is significantly affected by communication of the active site with a region dispensable for aminoacylation (*30*).

Discrimination at the transition state of catalysis was observed for several other AARSs as well. This discrimination involves specific protein–tRNA contacts at some distance from the catalytic active site. In the MetRS-catalyzed reaction, the anticodon of $tRNA^{Met}$ is a strong determinant for aminoacylation. Discrimination is achieved at the transition state with functional coupling between anticodon-binding and catalytic domains. Such coupling is evident in the aminoacylation kinetics of some tRNA and MetRS variants (Table II). In most cases, substitutions within the anticodon-binding domain of MetRS and the anticodon of $tRNA^{Met}$ significantly affected the Michaelis constant of the aminoacylation reaction, indicating that productive tRNA binding is impaired (*41*, *44*, *45*). However, substitution of the $tRNA^{Met}$ CAU anticodon with CCG did not significantly affect K_M, but reduced the k_{cat} for aminoacylation by 4 orders of magnitude (*46*). Similarly, mutations at Arg 395, which is within one of the α-helical peptides critical for binding the anticodon, reduced k_{cat} by 3 orders of magnitude (*47*). In contrast, K_M values were increased roughly 30-fold. It is likely that such changes reflect an induced-fit mechanism of tRNA recognition in this system (*48–50*).

Isoleucyl-tRNA synthetase (IleRS) recognizes a widely distributed set of identity elements for its isoaccepting tRNAs, including the anticodon (*51–53*). The major isoacceptor contains a GAU anticodon. Substitutions at the first position resulted in signficant decreases in k_{cat} for aminoacylation with minimal effects on K_M (*53*). Modified bases also play a role in the specificity of IleRS-catalyzed aminoacylation. An (unmodified) *in vitro* transcript of the major isoacceptor was aminoacylated with a k_{cat} that is reduced 400-fold relative to the mature tRNA. This was attributed primarily to a hypermodified carbamoylthreonine at position 37 (t^6A37) (*53*). The minor $tRNA_2^{Ile}$ isoacceptor contains an LAU anticodon, where L is lysidine (*54*). Just as with the major isoacceptor, aminoacylation (with IleRS) of an unmodified $tRNA_2^{Ile}$ was significantly impaired at the level of the transition state (*51*). These nucleotide determinants in the anticodon

loop likely affect the flexibility of $tRNA^{Ile}$. Indeed, chemical protection studies showed that binding by IleRS induced a conformational change in $tRNA^{Ile}$ (55). Given the long-range effects observed at the transition state of aminoacylation, a conformational change presumably presents the 3′ end of $tRNA^{Ile}$ in the active site for catalysis.

The archaebacterial *Methanococcus jannaschii* TyrRS differs from its bacterial counterpart by the absence of an anticodon-binding domain (Fig. 7) (56). Consistent with this observation was the determination that changes in the central nucleotide of the $tRNA^{Tyr}$ anticodon had only minimal effects on aminoacylation (57). The same substitutions substantially affect charging by the bacterial enzyme (58). A minihelix substrate based on the acceptor stem of *M. jannaschii* $tRNA^{Tyr}$ was specifically aminoacylated by the cognate TyrRS (57). Aminoacylation of the minihelix substrate, however, was diminished relative to aminoacylation of the full-length tRNA. This result suggested that contacts outside the minihelix arm were essential for efficient catalysis, despite the lack of a canonical anticodon-binding domain. Indeed, alanine substitutions at conserved residues (Asp 286 or Lys 288) within the shortened C-terminal domain significantly decreased the rate of $tRNA^{Tyr}$ aminoacylation (59). However, the catalytic core was not perturbed, as adenylate formation and minihelix aminoacylation were unaffected in the mutant enzymes compared to wild-type TyrRS. The defect in tRNA aminoacylation for the Asp286 → Ala substitution was entirely due to a 10-fold decrease in k_{cat} for aminoacylation, showing that communication occurs between even the shortened C-terminal domain and the catalytic site of *M. jannaschii* TyrRS (59).

Several viral RNAs fold into structures resembling tRNAs and are aminoacylated by AARSs (60, 61). Turnip yellow mosaic virus (TYMV), an example of a tRNA-like viral RNA, is aminoacylated by ValRS. Substitution studies

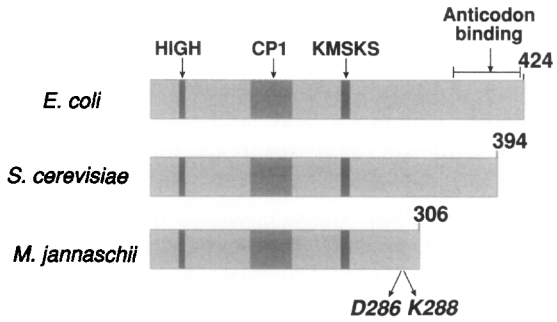

FIG. 7. *Methanococcus jannaschii* TyrRS lacks a typical anticodon-binding domain. Alanine substitutions at D286 and K288 demonstrated that domain–domain communication is necessary for efficient $tRNA^{Tyr}$ aminoacylation (59).

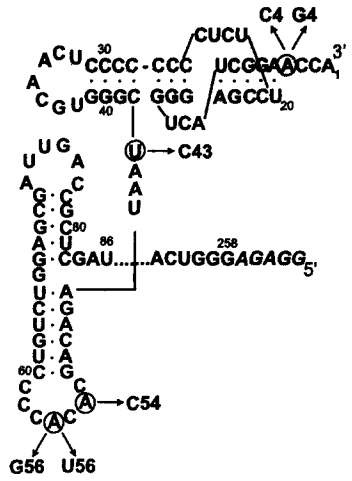

Transcript	K_M (μM)	V_m (arbitrary units)	Relative aminoacylation rate
TY-wt	0.21	100	1
TY-C4	0.25	4.1	0.034
TY-G4	1.00	1.4	3.0×10^{-3}
TY-C43	0.50	4.5	0.018
TY-C54	0.83	44	0.11
TY-G56	n.d.	n.d.	5.6×10^{-5}
TY-U56	n.d.	n.d.	3.6×10^{-5}

FIG. 8. Kinetic parameters for TYMV aminoacylation. The 3′ end of TYMV resembles tRNA, and aminoacylation by yeast ValRS is dependent on nucleotide identity within the acceptor-stem and anticodon mimics of the RNA (62).

demonstrated that nucleotides at the presumed anticodon, acceptor stem, and discriminator mimics were critical for valylation (Fig. 8). As shown for aminoacylation of tRNAs, specificity is determined by kinetic rather than binding effects. For example, substitutions at the central position of the anticodon mimic resulted in RNAs that were aminoacylated at a negligible rate (62). The variant RNAs nevertheless bound yeast ValRS with apparent K_ds nearly identical to that of the wild-type transcript. Furthermore, the anticodon-substituted variants were competitive inhibitors of the valylation of $tRNA^{Val}$ and of wild-type TYMV RNA by ValRS (62). Thus, the substitutions did not affect the enzyme–RNA interaction. In addition to substitutions at the anticodon, mutations in the variable loop region and at the discriminator position also had greater effects at the transition state than on binding. These observations, like the many examples of tRNA aminoacylation, point to a mechanism of long-range communication between catalytic and appended domains.

V. Understanding Communication Based on Structural Analysis

In contrast to the majority of synthetases, class I GlnRS, GluRS, and ArgRS require cognate tRNA for aminoacyl adenylate formation (2). Thus, the catalytic site for adenylate formation is not properly formed in the absence of tRNA, and tRNA binding triggers a rearrangement of the active site. Of the three enzymes, a crystal structure of the *E. coli* $tRNA^{Gln}$:GlnRS complex has been solved to 2.5 Å resolution (*63*). The structure revealed numerous contacts between $tRNA^{Gln}$ and GlnRS, and changes in the conformation of $tRNA^{Gln}$ when compared to the structures of free tRNAs (*64, 65*). Specifically, the anticodon stem is extended by two noncanonical base pairs, and the remaining three bases in the anticodon are splayed out to bind in three corresponding pockets of the enzyme (*66*). Furthermore, the acceptor stem is distorted from an A-form RNA helix, such that the first base pair (1:72) is unpaired, and the 3′ terminus bends back toward the stem to form a hairpin structure (Fig. 9).

These distortions at acceptor-stem and anticodon portions of $tRNA^{Gln}$ are stabilized (if not directly promoted) by protein domains outside the class I–defining Rossmann fold. The C-terminal half of GlnRS folds into two subdomains that together form a six-stranded antiparallel β-barrel (*63*). Residues at the junction of these subdomains form pockets responsible for discrimination of nucleotides in the $tRNA^{Gln}$ anticodon, located roughly 75 Å from the active site. In particular, U35 is held snugly by contacts with the side chains of five amino acids (*66*). At the other end of $tRNA^{Gln}$, a protein domain inserted between the

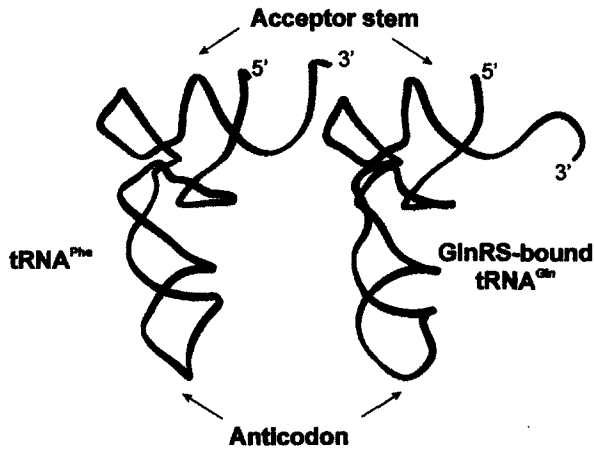

FIG. 9. Comparison of structures of free $tRNA^{Phe}$ (*64*) to enzyme-bound $tRNA^{Gln}$ (*63*). GlnRS binding produces distortions in the anticodon and acceptor stem of $tRNA^{Gln}$.

two halves of the nucleotide binding fold stabilizes the hairpin conformation of the acceptor stem (*63*). This recognition domain is a five-stranded antiparallel β-sheet flanked by three helices. The distorted conformation is stabilized by insertion of a β-loop between the 3′ and 5′ ends of $tRNA^{Gln}$, preventing reformation of the 1:72 base pair (*63*).

Determination of the cocrystal structure confirmed the importance for glutamine identity of nucleotides in the acceptor stem and anticodon. Substitution of these nucleotides affects primarily the k_{cat} for aminoacylation (*67*), showing that these contacts are necessary to present the 3′ end of the tRNA in the transition state. That substitutions at the anticodon have such large effects on k_{cat} argues for long-range communication between the anticodon-binding and catalytic domains (Table III).

In GlnRS (as well as GluRS and ArgRS), tRNA discrimination and adenylate formation are linked at the first step of aminoacylation. Therefore, domain–domain communication is manifested not only in the dependence of k_{cat} for aminoacylation, but also in the K_M for glutamine. For example, a C35 → G substitution in the anticodon resulted in a 30-fold decrease in k_{cat} and a 20-fold increase in K_M for glutamine (*68*). Likewise, an Arg341 → Ala substitution (in the anticodon-binding region of the protein) resulted in a nearly fourfold increase in the K_M for glutamine, with no effect on k_{cat} (*68*). The structural basis for this functional link was proposed to be a long two-stranded β-ribbon that extends from the two β-barrels of the anticodon-binding domain that packs against the active-site KMSKS motif (*66*). In the presence of cognate $tRNA^{Gln}$, this ribbon may transmit a signal to the active site domain, resulting in a productive conformation for catalysis.

TABLE III
KINETIC CONSTANTS FOR AMINOACYLATION OF $tRNA_2^{Gln}$ VARIANTS BY *E. coli* GlnRS

tRNA	K_M (μM)	k_{cat} (sec^{-1})	Relative aminoacylation (k_{cat}/K_M)
U1 (wild-type)	0.15	0.2	0.95
G1[a]	0.66	0.92	1.0
-U73	8.0	6.8×10^{-3}	6.0×10^{-4}
-G38	3.0	6.0×10^{-2}	1.4×10^{-2}
-U37	1.0	9.3×10^{-3}	6.6×10^{-3}
-A36	6.0	5.0×10^{-3}	5.9×10^{-4}
-C35	6.7	3.4×10^{-4}	3.6×10^{-5}
-A34	2.5	6.5×10^{-4}	1.9×10^{-4}

[a]Guanine substitution at the first position was a consequence of *in vitro* tRNA transcription using T7 RNA polymerase.

From Ref. *67*.

Functional determinants for aminoacylation of yeast $tRNA^{Asp}$ by AspRS are located principally at the discriminator base (G73) and the anticodon (GUC) (*69*). The structure of the yeast $tRNA^{Asp}$:AspRS complex was determined (*12, 70*) and revealed that specific contacts are made between tRNA identity elements and AspRS. Nucleotide substitutions at the discriminator base and at the conserved core of $tRNA^{Asp}$ affected the K_M of aminoacylation, likely due to removal of these required contacts. In contrast, substitutions at the anticodon were dominated by kinetic effects (*69*). For example, a G34C anticodon replacement increased K_M only 4-fold while decreasing k_{cat} 100-fold. Similar effects were observed at other anticodon positions (*69*). Clearly, nucleotides at the anticodon affect the orientation of the 3′ end of $tRNA^{Asp}$ and its presentation in the active site of the enzyme.

The cocrystal structure indeed revealed conformational changes in the tRNA upon enzyme binding (*12*). The acceptor end of $tRNA^{Asp}$ maintained a regular helical orientation (in contrast to the hairpin conformation of GlnRS-bound $tRNA^{Gln}$), although a modest change was observed at the three terminal base pairs. More significant was a distortion of the anticodon loop upon AspRS binding. The complexed $tRNA^{Asp}$ structure deviated from the free structure (*71*) beginning at base pair G30:U40, which seemed to act as a "hinge" point within the anticodon stem. In addition, the anticodon bases were unstacked upon complex formation. Recognition of these bases (three of the five identity elements within $tRNA^{Asp}$) is provided by seven amino acids within the N-terminal domain of AspRS (*70, 72*). Further mutational data supported the notion of functional coupling between tRNA determinants, with substitutions at the discriminator and anticodon (G35/A73 $tRNA^{Asp}$) resulting in cooperative losses in aminoacylation efficiency (Fig. 10) (*73*).

Several crystal structures of *Thermus thermophilus* SerRS have been determined, in isolation and with various substrates or analogs. This dimeric class II enzyme has several novel features. For example, SerRS does not contact the anticodon of $tRNA^{Ser}$. Instead, it recognizes the elongated variable arm though interaction with a helical motif at the enzyme's N terminus (*74*). Deletion of the N-terminal helical arm reduced the efficiency of aminoacylation 4 orders of magnitude relative to the full-length enzyme (*75*). Substitution of the long variable arm of type II $tRNA^{Ser}$ with a shorter type I tRNA loop reduced aminoacylation 3 orders of magnitude (*76*). A comparison of the uncomplexed synthetase with the SerRS:$tRNA^{Ser}$ complex (which also contained a nonhydrolyzable seryl adenylate analog) demonstrated that the helical arm is more flexible in the absence of cognate tRNA (*77*). Upon tRNA binding, this helical motif maximizes contacts with the variable arm and directs the acceptor stem into the active site for aminoacylation.

The most dramatic structural change in SerRS upon $tRNA^{Ser}$ binding is a switch in the conformation of the motif 2 loop. Because SerRS binds only one

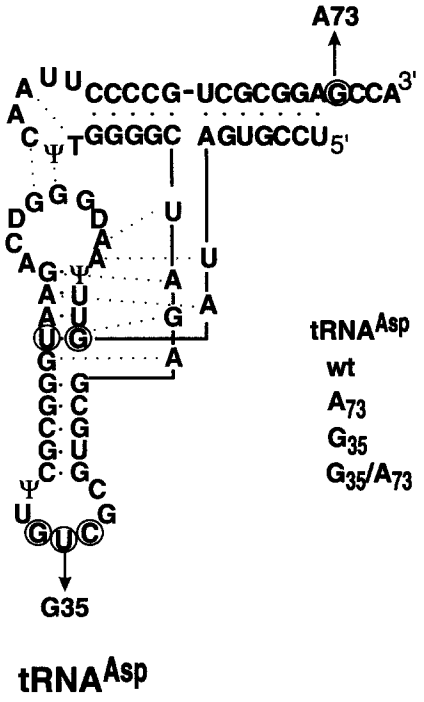

tRNA^{Asp}	k_{cat} (X10^{-3}/sec)	K_M (μM)	Activity Loss
wt	520	0.05	1
A_{73}	19	0.29	160
G_{35}	122	0.22	19
G_{35}/A_{73}	0.024	0.74	320,000

FIG. 10. Aminoacylation determinants (circled) of tRNA^{Asp}. Substitutions at G73 in the acceptor stem and U35 in the anticodon result in cooperative effects (*69*, *73*).

molecule of tRNA across the dimer interface, only one monomer has tRNA^{Ser} entering the active site, allowing direct comparisons between the tRNA-bound and unbound conformations. In the presence of ATP, or of the nonhydrolyzable adenylate analog, the loop adopts the previously observed "A conformation" (*78*), while tRNA binding induces a change to the "T conformation." These two orientations are mutually exclusive, stabilized by different interactions with the same set of conserved residues (*77*). In the absence of substrates, the motif 2 loop is disordered (*79*), demonstrating that different enzyme conformations are sampled as the aminoacylation reaction proceeds.

Indeed, other structural studies also identified conformational changes in AARSs, particularly in the active site, at various stages in the aminoacylation reaction. As further examples, conformational changes in either tRNA or protein have been documented in complexes between *T. thermophilus* LysRS and *E. coli* or *T. thermophilus* RNA^{Lys} (*80*), *E. coli* ThrRS and tRNA^{Thr} (*81*), and *E. coli* AspRS and tRNA^{Asp} (*82*); among others. Conformational changes were also predicted to occur upon adenylate formation in *Bacillus stearothermophilus* TrpRS (*83*).

The distortion of $tRNA^{Gln}$ upon *E. coli* GlnRS binding, which has already been discussed (*63*, *66*), was the model for a general evaluation of the conformational dynamics of complexes between tRNAs and AARSs (*84*). This study used a Gaussian network model (GNM) to predict flexibility and cooperative motions of both tRNA and AARS. In agreement with crystallographic data, GNM predictions identified the anticodon and acceptor stems exhibiting the highest structural flexibility. Nucleotides in the D and T arms and variable loops were determined to play crucial roles in global hinge-bending motions (*84*). Furthermore, invariant nucleotides were most highly restricted, as were conserved protein residues of GlnRS. Regions of the enzyme that demonstrated significant mobility, in contrast, were involved in the recognition of substrates (*84*).

VI. Communication by Conformational Changes in tRNA Studied in Solution

Given the abundance of structural data amassed in recent years, there should be evidence in solution for conformational changes that occur within cognate complexes. Indeed structural and kinetic studies raised the possibility that, in many cases, tRNA bound to its cognate AARS adopts a conformation distinct from that of tRNA in isolation. In this connection, early temperature-jump experiments investigating the $tRNA^{Ser}$-induced quenching of yeast SerRS fluorescence showed at least two relaxation processes. The results were consistent with a bimolecular reaction between the cognate partners and a conformational change of the complex (*85*). Fast kinetic studies extended these observations, comparing cognate and noncognate interactions for *E. coli* TyrRS, yeast SerRS, and *E. coli* and yeast PheRS (*86*, *87*). Together, the results led to the suggestion that tRNA discrimination occurs in two steps. In the first step, an AARS scans through many possible protein–tRNA interactions, transiently binding even noncognate tRNAs. This scanning occurs at diffusion-limited rates. In the second step, specific contacts with the cognate tRNA result in conformational changes within the complex that trigger selective aminoacylation. A simplified view of this proposed mechanism would attribute K_M contributions to the first step and k_{cat} contributions to the second, as these two parameters account for the specificity of aminoacylation (*42*).

The conformational flexibility of $tRNA^{Asp}$ was evident in I_2-footprinting experiments in the presence and absence of AspRS (*88*). Substitution of determinant nucleotides within the anticodon reduced protections within and outside of the anticodon loop, emphasizing the interdependence of contacts within the protein–RNA complex (*88*). This interdependence may correlate with long-range communication between anticodon and acceptor arms of $tRNA^{Asp}$,

particularly considering that substitutions in the anticodon affect primarily the k_{cat} parameter of aminoacylation (*69*).

Although a cocrystal structure is not available for the MetRS system, comparison of an early *E. coli* MetRS structure with the GlnRS structure predicted that $tRNA^{Met}$ would adopt a conformation similar to that of $tRNA^{Gln}$ when in complex with its cognate enzyme (*89*). Thus, as the observed hairpin conformation of the $tRNA^{Gln}$ acceptor stem was necessary for the 3′ end to reach the catalytic site for aminoacylation, such a distortion could be expected for $tRNA^{Met}$ as well.

An evaluation of $tRNA^{Met}$-derived microhelices determined that engineered destabilization at the first position of the acceptor stem resulted in enhanced aminoacylation by MetRS (*90*). A microhelix lacking the 5′-terminal nucleotide was aminoacylated at a rate 16-fold higher than the wild-type $microhelix^{Met}$ substrate. This enhancement corresponded to a reduction of 1.6 kcal/mol in the apparent free-energy barrier for transition-state formation. An enhancement of aminoacylation by IleRS was also observed for the 5′-truncated $minihelix^{Ile}$ construct (*90*). Although the engineered destabilization of the acceptor stem increased the rate of aminoacylation of both the $microhelix^{Met}$ and $minihelix^{Ile}$ substrates, addition of an anticodon stem-loop construct did not further enhance aminoacylation. If a distortion at the 3′ end of some tRNAs is a consequence of domain–domain communication, continuity of the tRNA backbone is essential.

VII. Communication in Aminoacylation That Requires Covalent Continuity of the tRNA Demonstrated by Functional Analysis

A well-studied example is the aminoacylation by MetRS of RNAs that recapitulate the acceptor stem of elongator and initiator $tRNAs^{Met}$. *E. coli* MetRS aminoacylates minihelices, microhelices, and duplexes with a catalytic efficiency that is reduced ~6 orders of magnitude relative to full-length $tRNA^{Met}$ (*91*, *92*). Such aminoacylation is sequence-specific, with substitutions in the acceptor stem decreasing aminoacylation in ways quantitatively similar to the reductions seen in the full-length substrate (*91*). The decrease in catalytic efficiency (k_{cat}/K_M) is not primarily due to a binding defect (Fig. 11). Gel-electrophoresis binding studies (*93*) determined that the apparent dissociation constant (K_d) for the MetRS:$microhelix^{fMet}$ interaction was decreased only ~20-fold compared to that for $tRNA^{fMet}$. Other microhelix constructs (either $microhelix^{fMet}$ variants or $microhelix^{Ala}$ substrates) bound with similar (or higher) affinities but were not methionylated by MetRS (*48*). Discrimination of the $microhelix^{fMet}$ substrate by MetRS therefore occurs in the transition state of catalysis.

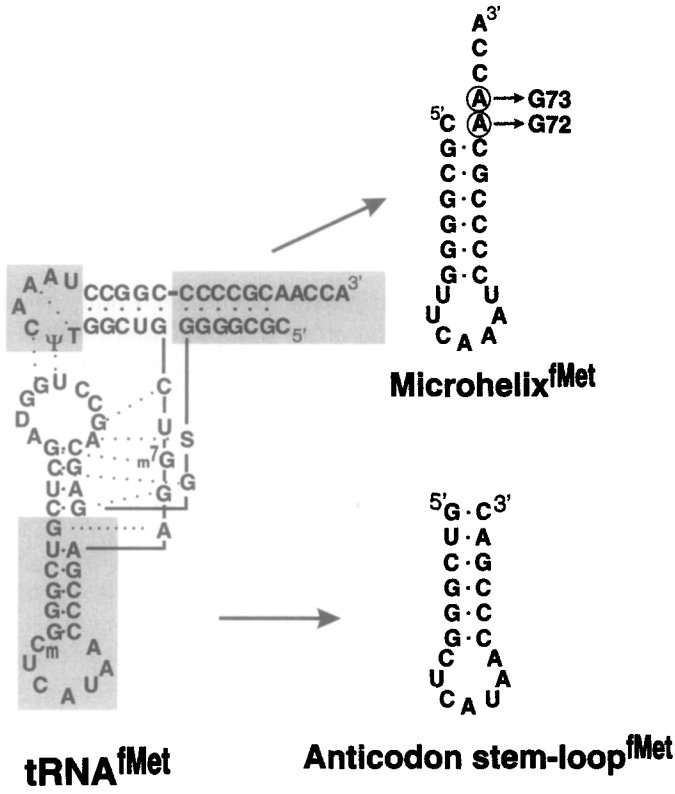

	K_d (μM)	Relative aminoacylation rate (k_{cat}/K_M)
tRNA^{fMet}	0.51 ± 0.14	1
Microhelix^{fMet}	12 ± 3	3.4 X 10^{-7}
G72, G73 Microhelix^{fMet}	12 ± 1	0.25 X 10^{-7}
Anticodon SL^{fMet}	22 ± 6	nd

FIG. 11. Stem–loop helices that recapitulate the arms of tRNA^{fMet}. Microhelix mimics of the tRNA^{fMet} acceptor arm are bound by MetRS and yet are aminoacylated at a low rate. An anticodon stem–loop hairpin is also bound by the enzyme but does not enhance microhelix aminoacylation (*48*). Domain–domain communication is dependent in this case upon covalent continuity of the tRNA backbone.

Binding of an isolated anticodon stem–loop hairpin to MetRS was also observed by affinity coelectrophoresis, with a K_d only 2-fold weaker than that of the microhelix (*48*). The anticodon stem–loop mimic bound MetRS in a manner similar to its binding in the context of the full $tRNA^{fMet}$, such that it was a competitive inhibitor of the $tRNA^{fMet}$ aminoacylation reaction (*94*). As stated earlier, addition of this anticodon stem–loop to the $microhelix^{fMet}$ aminoacylation reaction did not increase the efficiency of $microhelix^{fMet}$ charging (*90*). In some cases a slight increase in the rate of minihelix aminoacylation has been reported upon the addition of an anticodon fragment (*55, 95*), although the efficiency remained well below that of the corresponding full-length tRNA. Together, these results further suggested that efficient aminoacylation requires, at a minimum, communication that depends on covalent continuity between the acceptor stem and anticodon portions of tRNA.

VIII. Domain Communication in Editing

The ability of an AARS to discriminate between cognate and noncognate amino acids is limited primarily to binding interactions, and is more difficult when two substrates have similar structures. For example, valine differs from isoleucine by a single methylene group, while threonine and valine are isosteric. IleRS and ValRS, respectively, differentiate these noncognate from cognate amino acids using editing functions that are distinct from their aminoacylation activities. A "double-sieve" mechanism is thought to ensure amino acid selectivity (*96*). In the first sieve, amino acids larger than the cognate substrate are excluded from the catalytic active site, while smaller noncognate amino acids bind and are then hydrolyzed at a second active site for editing. This hydrolysis occurs either before (pretransfer) or after (posttransfer) attachment of the noncognate amino acid to tRNA (*97*). In the case of *E. coli* IleRS, misactivation of valine occurs at a rate approximately 1/180 that of isoleucine activation (*36*), but the $tRNA^{Ile}$-dependent editing reaction ensures that misincorporation of valine at isoleucine codons occurs with a frequency of less than 1 in 3000 (*98*).

$$\begin{array}{l} \text{IleRS} \cdot (\text{Val-AMP}) + \text{tRNA}^{\text{Ile}} \rightleftharpoons \text{IleRS} \cdot (\text{Val-AMP}) \cdot \text{tRNA}^{\text{Ile}} \rightleftharpoons \text{IleRS} \cdot (\text{Val-tRNA}^{\text{Ile}}) + \text{AMP} \\ \qquad\qquad\qquad\qquad\qquad\qquad \downarrow \text{Pretransfer editing} \qquad \downarrow \text{Posttransfer editing} \\ \qquad\qquad\qquad\qquad\qquad\qquad \text{IleRS} + \text{Val} + \text{AMP} + \text{tRNA}^{\text{Ile}} \qquad \text{IleRS} + \text{Val} + \text{AMP} + \text{tRNA}^{\text{Ile}} \end{array}$$

Biochemical and genetic studies showed that aminoacylation and editing functions of IleRS are contributed by distinct domains (*35, 36, 99*). A single mutation (Gly56 → Ala) in the IleRS catalytic site decreased discrimination for isoleucine over valine in the amino acid activation step (*36*). However,

posttransfer editing of Val-tRNA^{Ile} was unaffected by this mutation within the catalytic core. The location of the editing activity was identified by crosslinking a reactive analog of valine-misacylated tRNA^{Ile} (*N*-bromoacetyl-Val-tRNA^{Ile}) to IleRS (*35*). The misacylated analog crosslinked to connective polypeptide 1 (CP1, Fig. 4), an insertion that splits the catalytic domain between the third and fourth β-strands of the Rossmann fold (*35*, *100*). In contrast, the reactive Ile-tRNA^{Ile} analog crosslinked only to the active site. The structural and functional independence of the editing site was demonstrated by expression of the isolated CP1 domain, which efficiently deacylated Val-tRNA^{Ile} (*99*). Mutation or deletion of conserved residues within the CP1 domain severely diminished the editing activity of IleRS (*34*, *101–103*).

High-resolution crystal structures of IleRS from *T. thermophilus* (*101*) and *Staphylococcus aureus* (*104*) demonstrated that the structural domains are physically separate. The structure of *T. thermophilus* IleRS showed isoleucine bound to the conserved active site domain within the Rossmann fold. Valine bound to both the active site (for aminoacylation) and a second site within CP1. The editing and aminoacylation active sites are at least 25 Å apart (*101*, *104*), necessitating long-range communication between the active site and editing domains for efficient amino acid discrimination.

In parallel with the distinct domains responsible for aminoacylation and editing activities of IleRS, RNA determinants for the two functions are separate. The anticodon of tRNA^{Ile} is a major identity element for aminoacylation by IleRS (*51*, *53*). Small RNA substrates (minihelices and microhelices) of tRNA^{Ile} are aminoacylated (albeit inefficiently) in a sequence-specific manner. Thus, determinants for isoleucinylation are also contained in the acceptor stem (*55*, *90*). In contrast, nucleotides in the D loop of tRNA^{Ile} trigger the editing reaction of IleRS (Fig. 12) (*105–107*). Replacement of G16, D20, and G21 with their tRNA^{Val} counterparts abolished the editing response in the presence of valine and tRNA^{Ile}. However, these substitutions had no effect on aminoacylation with isoleucine (*105*). Each of the three nucleotides contributed to the editing response, because any substitution at these positions adversely affected the editing activity (*106*).

Substitutions in the D loop of tRNA^{Ile} that affect editing do not decrease binding to IleRS, as determined by gel retardation assays (*106*). Indeed, the D loop is thought not to make contact with IleRS, as nucleotides essential for editing are not protected from chemical modification in the presence of the enzyme (*53*). A conformational change in tRNA^{Ile}, mediated by nucleotides in the D loop, may be responsible for inducing editing by IleRS. Furthermore, this conformational change must involve a form of domain–domain communication. For example, when a minihelix is mixed with the D loop–containing domain of tRNA^{Ile}, no editing of misactivated adenylate occurs. Thus, covalent continuity of the tRNA is required for the domain–domain communication.

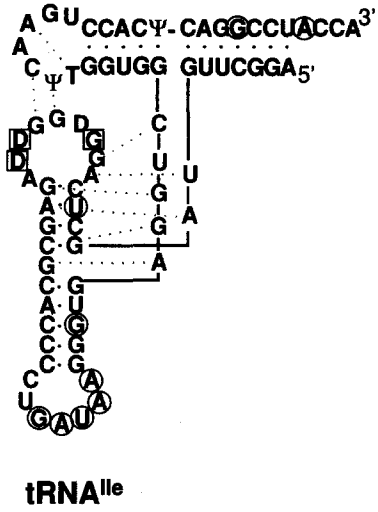

FIG. 12. Aminoacylation and editing determinants of $tRNA^{Ile}$. Nucleotides critical for aminoacylation by IleRS are circled (*53*), while those required for IleRS editing activity are boxed (*105*).

The crystal structure of *S. aureus* IleRS with bound $tRNA^{Ile}$ (and the antibiotic mupirocin) revealed an editing complex structurally distinct from the expected catalytic conformation. Although the 3′ end of $tRNA^{Ile}$ was disordered, the remaining structure dictated that the acceptor terminus be an A-form helix that makes a direct path into the editing active site (*104*). In contrast, comparison of the structures of uncomplexed IleRS (*101*) and a $tRNA^{Gln}$:GlnRS complex (*63*) predicted that the 3′ end of $tRNA^{Ile}$ must be distorted to access the catalytic active site for aminoacylation (Fig. 13). Other $tRNA^{Ile}$:IleRS contacts were different from those predicted to occur in the catalytic complex. For example, within the class I–conserved K^{595}MSKS peptide, the backbone amide of Lys 595 and the backbone carbonyl of Gly 593 bound to the tRNA backbone, stabilizing the extended conformation of the 3′ end (*104*). The KMSKS sequence of the ligand-free IleRS was in a different conformation, suggesting that tRNA binding induced the structural change.

Other evidence suggested a tRNA-induced conformational change in IleRS leading to editing. A DNA aptamer able to trigger hydrolysis of Val-AMP demonstrated that editing could be achieved independently of aminoacylation (*108*). The DNA aptamer lacked the terminal 2′-OH necessary for aminoacylation by IleRS and previously thought to be required as a "tentative acceptor" in the editing reaction (*109, 110*). The aptamer could not be folded into a tRNA-like structure and bore no particular sequence similarity to $tRNA^{Ile}$ (*108*). A reactive aptamer crosslinked to the CP1 region of IleRS (*111*).

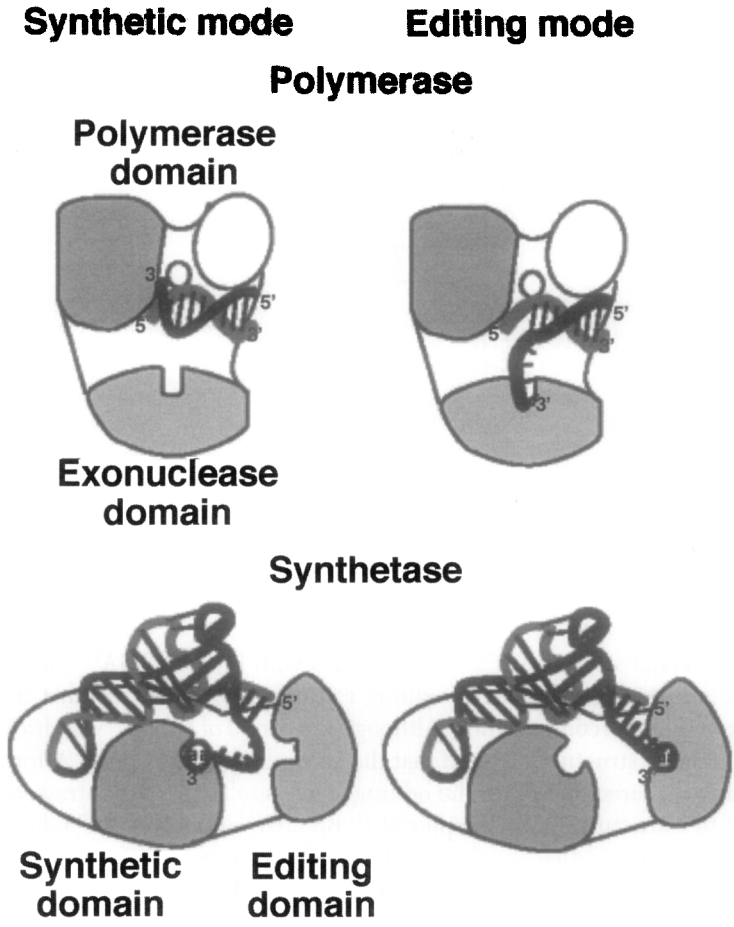

FIG. 13. Translocation between catalytic and editing sites in two systems. The 3′ end of DNA lies in the polymerase active site for replication and shifts to the exonuclease site for removal of misincorporated nucleotides. Similarly, the 3′ end of tRNA translocates between the IleRS catlytic and editing sites. However, it is not clear whether this mechanism can explain pretransfer editing, where the misactivated adenylate shuttles from the active site to the editing site. Reprinted with permission from Ref. *104*. Copyright 1999 American Association for the Advancement of Science.

Editing of misactivated amino acid (whether isolated or attached to tRNA) requires two steps: translocation to the editing site and chemical hydrolysis. Energy transfer experiments using a fluorescent analog of ATP demonstrated that translocation is the rate-limiting step for editing (*103*). Furthermore, D-loop nucleotides G16, D20, and D21 are important for translocation. Substitution of these nucleotides within the context of $tRNA^{Ile}$ did not affect the hydrolysis

of misacylated Val-tRNA^{Ile} (*106*). A minihelix^{Ile} (which lacked the D-loop determinants for editing) was misacylated with valine because of a defect in the translocation step (*107*). The efficiency of the DNA aptamer described above may lie, therefore, in its ability to trigger the translocation step of pretransfer editing and properly position the adenylate for enzyme-catalyzed hydrolysis.

IX. Role of Induced Fit

Together, the confomational changes observed in both AARS and tRNA components of the aminoacylation and editing reactions suggest that domain–domain communication proceeds through an induced-fit mechanism. As proposed by Koshland (*112*, *113*), induced fit occurs when binding of a substrate causes a conformational change in the enzyme to align the catalytic groups properly. In RNA–protein complexes, structural changes are often seen in both protein and RNA components upon binding (*114*). For example, the U1A protein regulates its polyadenylation by binding a loop in the 3′-untranslated region (UTR) of its mRNA. Upon binding, the C-terminal helix of U1A swings away from the face of the protein to allow close contacts with the mRNA loop. The RNA loop also shows altered nucleotide stacking interactions, demonstrating the mutually induced fit of the complex (*115*). Ribosomal proteins also have been shown to bind RNA (either rRNA or their own mRNA) through a mutually induced fit mechanism (*114*).

Similarly, most conformational changes observed upon AARS:tRNA complex formation occur in both protein and RNA components. In addition to the examples cited above, several additional cases can be cited. These include examples from structural analysis as well as investigations in solutions. A comparison of the tRNA^{Pro}-bound ProRS (from *T. thermophilus*) with its unbound counterpart indicated conformational flexibility in the isolated enzyme (*116*). Most significant was a hinge movement of the anticodon-binding domain in relation to the catalytic domain. Also, several loops near the active site were less tightly constrained in the absence of small substrates (either prolyl adenylate or a nonhydrolyzable analog). In contrast, the β-sheet making up the catalytic core of the enzyme was rigid even in the isolated enzyme, as was the C-terminal zinc-binding domain (*116*).

The tRNA^{Pro} in complex with ProRS was bound in a noncatalytic orientation, as the acceptor end was disordered and not in the enzyme active site (*116*). The only enzyme–tRNA contact was at the anticodon, which was distorted relative to the structure of uncomplexed tRNA^{Phe}. An active ProRS:tRNA^{Pro} complex was modeled based on the crystal structure of the closely related class IIa ThrRS:tRNA^{Thr} complex from *E. coli* (*81*). In order for the acceptor stem of tRNA^{Pro} to reach the ProRS active site, a significant change in the tRNA

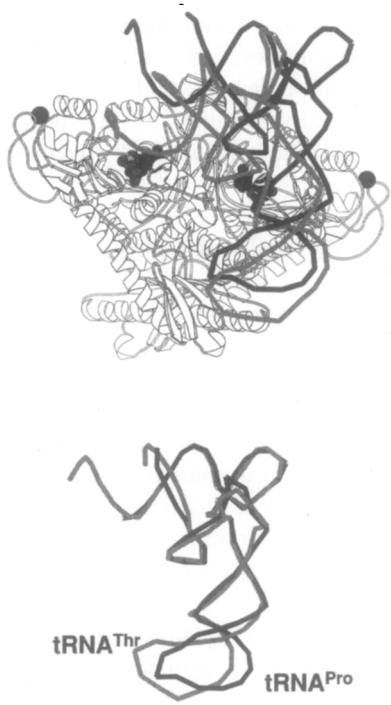

FIG. 14. Structural comparison of $tRNA^{Thr}$ and $tRNA^{Pro}$ in enzyme-bound conformations. Top: $tRNA^{Thr}$ superimposed on *Thermus thermophilus* ProRS:$tRNA^{Pro}$:ProAMS ternary complex (*116*). The two monomers of ProRS are outlined in gray and black, and the $tRNA^{Pro}$ backbone is black. ProAMS, a nonhydrolyzable prolyl adenylate analog, is located in the enzyme active site. The position of $tRNA^{Thr}$ (gray) is that from its complex with *E. coli* ThrRS (*81*), with the catalytic domains of ThrRS (not shown) and ProRS aligned. The ThrRS:$tRNA^{Thr}$ complex is in a catalytically productive conformation, while the 3′ end of $tRNA^{Pro}$ (black) is disordered and would require a significant conformational change to reach the enzyme active site. Bottom: The overall conformations of enzyme-bound $tRNA^{Thr}$ and $tRNA^{Pro}$ are similar, except at the anticodon loops. Figure kindly provided by Dr. Stephen Cusack.

conformation was demonstrated to be necessary (Fig. 14). This may be the result of a reorientation of the anticodon-binding domain relative to the catalytic domain or of other protein-induced changes in the $tRNA^{Pro}$ structure, perhaps upon adenylate formation (*116*). Thus the catalytically active ProRS:$tRNA^{Pro}$ complex differs structurally from its isolated components.

The recent structure of the ternary yeast ArgRS:$tRNA^{Arg}$:L-arginine complex provides further insight into conformational changes leading to domain–domain communication (*117*). Comparison with the "tRNA-free" yeast ArgRS structure (*118*) revealed significant distortions in the anticodon loop and acceptor end

of $tRNA^{Arg}$, as has been seen for other enzyme-bound tRNAs (*63, 81, 116*). Recognition of the anticodon loop by ArgRS involves formation of a bulge at A38, intercalation of A37 into the last base pair of the anticodon stem, and the splaying out of anticodon bases U33, I34, and C35. Conserved residues in the ArgRS anticodon-binding domain stabilize this conformation of the loop. For example, all ArgRS sequences end in methionine, which is Met 607 in the yeast enzyme. This methionine interacts with G36 and A38 in the distorted conformation of the loop.

The 3′ end of $tRNA^{Arg}$ forms a hairpin structure to access the catalytic site of the enzyme, similar to that previously observed for enzyme-bound $tRNA^{Gln}$ (*63*). However, the molecular mechanisms used are different in each case. The terminal base pair (Ψ1:A72) of $tRNA^{Arg}$ remains paired, and the hairpin is stabilized by enzyme interactions with C74 and A76.

Communication between the anticodon-binding and catalytic domains of yeast ArgRS is mediated through conformational changes in two helices (H15 and H6) that link together the domains. A helix (H15) encompassing Phe 417 to Lys 435 forms one side of the pocket recognizing G36 and G38, and is conformationally altered upon tRNA binding. Structural changes in helix H15 induce changes in the class I HIGH and KMSKS signature peptides (in yeast ArgRS the corresponding residues are H_{159}AHG and M_{408}STR). Thus, upon tRNA binding, the MSTR loop flips and the helix (H6) containing HAHG moves to produce a more open active site. This may be the structural basis for ArgRS's requirement for $tRNA^{Arg}$ binding prior to aminoacyl adenylate formation.

Furthermore, comparison of the binary complex (lacking arginine) with the ternary complex revealed that amino acid binding triggers the proper orientation of the tRNA CCA end. When arginine is bound, the conserved Tyr 347 interacts with both the amino acid and the adenine ring of A76, continuing the stacking interaction of A76 and C75 in the hairpin conformation. In the absence of arginine, Tyr 347 is hydrogen-bonded to the carbonyl of Trp192 and does not contact A76. In the binary complex, therefore, the tRNA CCA end is disordered, and the position of G73 suggests that the acceptor stem maintains its helical conformation rather than forming the productive hairpin structure. Thus, both $tRNA^{Arg}$ and arginine binding induce conformational changes that result in a catalytically competent conformation of ArgRS. These changes are mediated by the long helix H15 that serves as a structural link between anticodon-binding and active-site domains, and by conserved residues in the active site that are conformationally flexible (*117*).

Experimental evidence suggests that some substrate binding energy may be used to disrupt the AARS and/or tRNA conformation, as predicted by Fersht (*97*). For example, comparison of the crystal structures of ligand-free *B. stearothermophilus* TyrRS and its tyrosyl adenylate complex revealed a conformational change in the enzyme active site upon adenylate formation (*119*).

Kinetic studies of TyrRS mutants evaluated the energy levels of the reaction intermediates to predict how particular residues interact with components of the activation step (tyrosine, ATP, the transition state, adenylate-PP_i, and adenylate) (*120*). This analysis revealed that Lys 82, Arg 86, Lys 230, and Lys 233 interacted with the transition state of activation, despite their distance from the active site in the crystal structure of the free enzyme. Indeed, these residues were localized to two flexible loops in the catalytic domain (*119*). In an induced-fit mechanism, the loops were proposed to wrap around the pyrophosphate portion of ATP upon tyrosine binding, then open again once the adenylate was formed (*120*).

Binding energies for the acceptor helix and anticodon arms of $tRNA^{fMet}$ in complex with MetRS have been determined based on affinity coelectrophoresis analysis (*93*). The sum of free energies of binding for the two arms was much higher (by 7 kcal/mol) than for the full-length $tRNA^{fMet}$. Much of this difference may be the cost associated with distorting the tRNA upon binding to MetRS. Furthermore, binding and activation energies were compared for $microhelix^{fMet}$ and $tRNA^{fMet}$. Whereas the difference in apparent free energy of activation was calculated to be 9.2 kcal/mol, binding differed by only 1.9 kcal/mol (*48*). For the more active tRNA substrate, then, some or all of the energy cost associated with strain of the tRNA upon binding may result in a conformation of the enzyme:tRNA complex that more closely resembles the transition state of catalysis. This may be manifest in the elevated k_{cat} for aminoacylation of $tRNA^{fMet}$ (compared to the microhelix) because of the reduced activation energy barrier (*48*). A portion of this reduction was achieved by engineering a destabilization in the acceptor stem of $microhelix^{fMet}$ (*90*).

Additionally, mutations of MetRS in two of the helices known to be involved in anticodon binding showed that induced fit of $tRNA^{fMet}$ could be interrupted without affecting adenylate formation, microhelix aminoacylation, or anticodon binding (*50*). Alanine substitutions at Asn 387 and Asn 452 resulted in a variant enzyme with significantly decreased binding and aminoacylation of $tRNA^{fMet}$. Yet the microhelix and anticodon arms in isolation bound the double mutant with affinities approximately equivalent to those with the wild-type enzyme, as evidenced by identical microhelix aminoacylation rates and inhibition of $tRNA^{fMet}$ aminoacylation by anticodon stem–loop helices, respectively (*50*). Amino acids in a domain distinct from the catalytic core reduced aminoacylation because the binding energies of the individual tRNA arms could not be converted into the conformational change necessary to produce the active AARS:tRNA complex.

As described above, residues in the C-terminal half of *E. coli* MetRS are responsible for recognition of the CAU anticodon of $tRNAs^{Met}$. A genetic study showed that several residues in the anticodon-recognizing helix–loop peptide (Lys 439 to Gly 468) could be substituted with little effect on enzyme activity, while a small number of residues (Asn 452, Arg 453, Pro 460, Trp 461, and Lys 465) were invariant (*121, 122*). Molecular dynamics simulations carried out

on both active and inactive variants of the peptide demonstrated that inactivity correlated with increased flexibility of the peptide (*49*). This result suggested that the difference between inactive and active variants of the enzyme (in some cases differing by a single residue) was the result of the increased energy required to constrain the RNA-binding region of the protein. If indeed induced fit is utilized in AARS:tRNA complex formation, fixation of the residues at the tRNA binding site may reduce the entropic cost of the induced-fit mechanism.

Induced fit has been demonstrated for other tRNA-binding enzymes. Methionyl-tRNA formyltransferase (MTF) is essential for generating the formylated version of Met-tRNA^{fMet} recognized as the initiator tRNA in bacterial and organellar protein synthesis (*123*). The crystal structure of *E. coli* MTF revealed its domain organization, with an N-terminal domain highly homologous to glycinamide ribonuclotide formyltransferase, another formylating enzyme. The C-terminal domain of MTF was proposed to make nonspecific contacts with tRNA^{fMet}. As with some AARSs, the two domains of MTF are linked by a peptide loop (*124*). The peptide was flexible enough to be disordered in the crystal structure, and was susceptible to protease cleavage in the absence of tRNA. In contrast, formation of an active complex between MTF and tRNA^{fMet} protected the peptide loop from cleavage (*125*). Protection did not occur when the complex contained mutations (in either MTF or tRNA^{fMet}) known to inhibit formylation. Apparent dissociation constants of the variant MTF:tRNA^{fMet} complexes were largely unchanged relative to interaction between wild-type components, demonstrating again that specificity is achieved at the catalytic (rather than binding) step. A cocrystal structure of the complex between MTF and fMet-tRNA^{fMet} revealed that tRNA binding did indeed cause a conformational change in the peptide linker (*126*). In the case of MTF, therefore, catalysis is achieved through an induced-fit mechanism in which tRNA is the activating substrate. Binding of AA-tRNA has also been proposed to trigger a conformational change in the decoding center of 16S ribosomal RNA, in an induced-fit mechanism for substrate selection at the ribosome (*127*).

X. Conclusion

One of the key early questions in the investigation of the aminoacylation reaction was the tRNA identity elements recognized by individual AARSs. Much has been worked out in this area through genetic, chemical, and kinetic studies (*45, 128*). Strides have also been made in structure determinations, such that comparisons of ligand-free and liganded AARSs can be compared, as can isofunctional enzymes from different organisms. One outstanding challenge is a detailed description of the molecular mechanism of aminoacylation and editing. This will require further structural studies, including descriptions of enzymes

in the presence of substrates, transition-state analogs, and inhibitors. But it is important also to revisit some of the early kinetic work that sought to understand tRNA discrimination on a fast time scale (85–87). With the tools and techniques now available, comparisons of structural changes occurring in the presence of cognate, noncognate, and near-cognate tRNAs (including tRNA pieces) may further enlighten the basis for domain–domain communication in AARSs. Finally, because these enzymes are intimately linked to the origin of life, the evolution of tRNA synthetase structure remains an important problem for the future. This evolution is inseparable from consideration of the evolution of tRNA and the full development of the universal genetic code. During this long evolution, domain–domain communication played an essential role.

ACKNOWLEDGMENTS

This work was supported by grants GM15539 and 23562 from the National Institutes of Health and by a fellowship from the National Foundation for Cancer Research.

REFERENCES

1. P. R. Schimmel and D. Söll, *Annu. Rev. Biochem.* **48,** 601 (1979).
2. D. Söll and P. Schimmel, *Enzymes* **10,** 489 (1974).
3. A. Rich, *in* "Horizons in Biochemistry" (M. Kasha and B. Pullman, eds.), p. 103. Academic Press, New York, 1962.
4. C. R. Woese, *in* "Organization and Control of Prokaryotic and Eukaryotic cells: 20th Symposium of the Society for General Microbiology" (H. P. Charles and B. C. J. G. Knight, eds.), p. 39. Cambridge University Press, London, 1970.
5. G. M. Nagel and R. F. Doolittle, *J. Mol. Evol.* **40,** 487 (1995).
6. T. Webster, H. Tsai, M. Kula, G. A. Mackie, and P. Schimmel, *Science* **226,** 1315 (1984).
7. S. W. Ludmerer and P. Schimmel, *J. Biol. Chem.* **262,** 10801 (1987).
8. G. Eriani, M. Delarue, O. Poch, J. Gangloff, and D. Moras, *Nature (London)* **347,** 203 (1990).
9. S. Cusack, C. Berthet-Colominas, M. Hartlein, N. Nassar, and R. Leberman, *Nature (London)* **347,** 249 (1990).
10. S. T. Rao and M. G. Rossmann, *J. Mol. Biol.* **76,** 241 (1973).
11. C. Hountondji, F. Lederer, P. Dessen, and S. Blanquet, *Biochemistry* **25,** 16 (1986).
12. M. Ruff, S. Krishnaswamy, M. Boeglin, A. Poterszman, A. Mitschler, A. Podjarny, B. Rees, J. C. Thierry, and D. Moras, *Science* **252,** 1682 (1991).
13. M. Ibba, S. Morgan, A. W. Curnow, D. R. Pridmore, U. C. Vothknecht, W. Gardner, W. Lin, C. R. Woese, and D. Söll, *Science* **278,** 1119 (1997).
14. P. Schimmel, R. Giegé, D. Moras, and S. Yokoyama, *Proc. Natl. Acad. Sci. U.S.A.* **90,** 8763 (1993).
15. M. Delarue and D. Moras, *Bioessays* **15,** 675 (1993).
16. S. D. Putney, R. T. Sauer, and P. R. Schimmel, *J. Biol. Chem.* **256,** 198 (1981).
17. M. Jasin, L. Regan, and P. Schimmel, *Nature (London)* **306,** 441 (1983).

18. C. Ho, M. Jasin, and P. Schimmel, *Science* **229,** 389 (1985).
19. S. J. Park and P. Schimmel, *J. Biol. Chem.* **263,** 16527 (1988).
20. Y. M. Hou and P. Schimmel, *Nature (London)* **333,** 140 (1988).
21. W. H. McClain and K. Foss, *Science* **240,** 793 (1988).
22. C. Francklyn and P. Schimmel, *Nature (London)* **337,** 478 (1989).
23. S. J. Park, Y. M. Hou, and P. Schimmel, *Biochemistry* **28,** 2740 (1989).
24. K. Musier-Forsyth, N. Usman, S. Scaringe, J. Doudna, R. Green, and P. Schimmel, *Science* **253,** 784 (1991).
25. D. D. Buechter and P. Schimmel, *Biochemistry* **32,** 5267 (1993).
26. N. Y. Sardesai and P. Schimmel, *J. Amer. Chem. Soc.* **120,** 3269 (1998).
27. L. Ribas de Pouplana, D. Buechter, N. Y. Sardesai, and P. Schimmel, *EMBO J.* **17,** 5449 (1998).
28. L. Regan, J. Bowie, and P. Schimmel, *Science* **235,** 1651 (1987).
29. Y. M. Hou and P. Schimmel, *Biochemistry* **31,** 10310 (1992).
30. M. Jasin, L. Regan, and P. Schimmel, *J. Biol. Chem.* **260,** 2226 (1985).
31. S. Kim and P. Schimmel, *J. Biol. Chem.* **267,** 15563 (1992).
32. S. Kim, J. A. Landro, A. J. Gale, and P. Schimmel, *Biochemistry* **32,** 13026 (1993).
33. A. Shepard, K. Shiba, and P. Schimmel, *Proc. Natl. Acad. Sci. U.S.A.* **89,** 9964 (1992).
34. T. L. Hendrickson, T. K. Nomanbhoy, and P. Schimmel, *Biochemistry* **39,** 8180 (2000).
35. E. Schmidt and P. Schimmel, *Biochemistry* **34,** 11204 (1995).
36. E. Schmidt and P. Schimmel, *Science* **264,** 265 (1994).
37. J. J. Burbaum and P. Schimmel, *Biochemistry* **30,** 319 (1991).
38. K. Shiba and P. Schimmel, *Proc. Natl. Acad. Sci. U.S.A.* **89,** 1880 (1992).
39. K. Shiba and P. Schimmel, *J. Biol. Chem.* **267,** 22703 (1992).
40. S. Blanquet, M. Iwatsubo, and J. P. Waller, *Eur. J. Biochem.* **36,** 213 (1973).
41. T. Meinnel, Y. Mechulam, D. Le Corre, M. Panvert, S. Blanquet, and G. Fayat, *Proc. Natl. Acad. Sci. U.S.A.* **88,** 291 (1991).
42. J. P. Ebel, R. Giegé, J. Bonnet, D. Kern, N. Befort, C. Bollack, F. Fasiolo, J. Gangloff, and G. Dirheimer, *Biochimie* **55,** 547 (1973).
43. M. Jasin, L. Regan, and P. Schimmel, *Cell (Cambridge, Mass.)* **36,** 1089 (1984).
44. G. Ghosh, H. Pelka, and L. H. Schulman, *Biochemistry* **29,** 2220 (1990).
45. L. H. Schulman, *Prog. Nucleic Acid Res. Mol. Biol.* **41,** 23 (1991).
46. L. H. Schulman and H. Pelka, *Science* **246,** 1595 (1989).
47. H. Y. Kim, H. Pelka, S. Brunie, and L. H. Schulman, *Biochemistry* **32,** 10506 (1993).
48. A. J. Gale, J. P. Shi, and P. Schimmel, *Biochemistry* **35,** 608 (1996).
49. L. Ribas de Pouplana, D. S. Auld, S. Kim, and P. Schimmel, *Biochemistry* **35,** 8095 (1996).
50. R. W. Alexander and P. Schimmel, *Biochemistry* **38,** 16359 (1999).
51. T. Muramatsu, K. Nishikawa, F. Nemoto, Y. Kuchino, S. Nishimura, T. Miyazawa, and S. Yokoyama, *Nature (London)* **336,** 179 (1988).
52. L. Pallanck and L. H. Schulman, *Proc. Natl. Acad. Sci. U.S.A.* **88,** 3872 (1991).
53. O. Nureki, T. Niimi, T. Muramatsu, H. Kanno, T. Kohno, C. Florentz, R. Giegé, and S. Yokoyama, *J. Mol. Biol.* **236,** 710 (1994).
54. T. Muramatsu, S. Yokoyama, N. Horie, A. Matsuda, T. Ueda, Z. Yamaizumi, Y. Kuchino, S. Nishimura, and T. Miyazawa, *J. Biol. Chem.* **263,** 9261 (1988).
55. O. Nureki, T. Niimi, Y. Muto, H. Kanno, T. Kohno, T. Muramatsu, G. Kawai, T. Miyazawa, R. Giegé, C. Florentz, and S. Yokoyama, *in* "The Translational Apparatus" (K. H. Nierhaus, F. Franceschi, A. R. Subramanian, V. A. Erdmann, and B. Wittmann-Liebold, eds.), p. 59. Plenum Press, New York, 1993.
56. T. A. Kleeman, D. Wei, K. L. Simpson, and E. A. First, *J. Biol. Chem.* **272,** 14420 (1997).

57. B. A. Steer and P. Schimmel, *J. Biol. Chem.* **274,** 35601 (1999).
58. H. Himeno, T. Hasegawa, T. Ueda, K. Watanabe, and M. Shimizu, *Nucleic Acids Res.* **18,** 6815 (1990).
59. B. A. Steer and P. Schimmel, *Proc. Natl. Acad. Sci. U.S.A.* **96,** 13644 (1999).
60. R. Giegé, *Proc. Natl. Acad. Sci. U.S.A.* **93,** 12078 (1996).
61. R. Giegé, C. Florentz, and T. W. Dreher, *Biochimie* **75,** 569 (1993).
62. C. Florentz, T. W. Dreher, J. Rudinger, and R. Giegé, *Eur. J. Biochem.* **195,** 229 (1991).
63. M. A. Rould, J. J. Perona, D. Söll, and T. A. Steitz, *Science* **246,** 1135 (1989).
64. S. H. Kim, F. L. Suddath, G. J. Quigley, A. McPherson, J. L. Sussman, A. H. Wang, N. C. Seeman, and A. Rich, *Science* **185,** 435 (1974).
65. J. D. Robertus, J. E. Ladner, J. T. Finch, D. Rhodes, R. S. Brown, B. F. Clark, and A. Klug, *Nature (London)* **250,** 546 (1974).
66. M. A. Rould, J. J. Perona, and T. A. Steitz, *Nature (London)* **352,** 213 (1991).
67. M. Jahn, M. J. Rogers, and D. Söll, *Nature (London)* **352,** 258 (1991).
68. M. Ibba, K. W. Hong, J. M. Sherman, S. Sever, and D. Söll, *Proc. Natl. Acad. Sci. U.S.A.* **93,** 6953 (1996).
69. J. Putz, J. D. Puglisi, C. Florentz, and R. Giegé, *Science* **252,** 1696 (1991).
70. J. Cavarelli, B. Rees, M. Ruff, J. C. Thierry, and D. Moras, *Nature (London)* **362,** 181 (1993).
71. E. Westhof, P. Dumas, and D. Moras, *J. Mol. Biol.* **184,** 119 (1985).
72. J. Cavarelli, B. Rees, J. C. Thierry, and D. Moras, *Biochimie* **75,** 1117 (1993).
73. J. Putz, J. D. Puglisi, C. Florentz, and R. Giegé, *EMBO J.* **12,** 2949 (1993).
74. V. Biou, A. Yaremchuk, M. Tukalo, and S. Cusack, *Science* **263,** 1404 (1994).
75. F. Borel, C. Vincent, R. Leberman, and M. Hartlein, *Nucleic Acids Res.* **22,** 2963 (1994).
76. J. R. Sampson and M. E. Saks, *Nucleic Acids Res.* **21,** 4467 (1993).
77. S. Cusack, A. Yaremchuk, and M. Tukalo, *EMBO J.* **15,** 2834 (1996).
78. H. Belrhali, A. Yaremchuk, M. Tukalo, C. Berthet-Colominas, B. Rasmussen, P. Bosecke, O. Diat, and S. Cusack, *Structure* **3,** 341 (1995).
79. M. Fujinaga, C. Berthet-Colominas, A. D. Yaremchuk, M. A. Tukalo, and S. Cusack, *J. Mol. Biol.* **234,** 222 (1993).
80. S. Cusack, A. Yaremchuk, and M. Tukalo, *EMBO J.* **15,** 6321 (1996).
81. R. Sankaranarayanan, A. C. Dock-Bregeon, P. Romby, J. Caillet, M. Springer, B. Rees, C. Ehresmann, B. Ehresmann, and D. Moras, *Cell (Cambridge, Mass.)* **97,** 371 (1999).
82. S. Eiler, A. Dock-Bregeon, L. Moulinier, J. C. Thierry, and D. Moras, *EMBO J.* **18,** 6532 (1999).
83. V. A. Ilyin, B. Temple, M. Hu, G. Li, Y. Yin, P. Vachette, and C. W. Carter, Jr., *Protein Sci.* **9,** 218 (2000).
84. I. Bahar and R. L. Jernigan, *J. Mol. Biol.* **281,** 871 (1998).
85. R. Rigler, U. Pachmann, R. Hirsch, and H. G. Zachau, *Eur. J. Biochem.* **65,** 307 (1976).
86. G. Krauss, D. Riesner, and G. Maass, *Eur. J. Biochem.* **68,** 81 (1976).
87. D. Riesner, A. Pingoud, D. Boehme, F. Peters, and G. Maass, *Eur. J. Biochem.* **68,** 71 (1976).
88. J. Rudinger, J. D. Puglisi, J. Pütz, D. Schatz, F. Eckstein, C. Florentz, and R. Giegé, *Proc. Natl. Acad. Sci. U.S.A* **89,** 5882 (1992).
89. J. J. Perona, M. A. Rould, T. A. Steitz, J. L. Risler, C. Zelwer, and S. Brunie, *Proc. Natl. Acad. Sci. U.S.A.* **88,** 2903 (1991).
90. R. W. Alexander, B. E. Nordin, and P. Schimmel, *Proc. Natl. Acad. Sci. U.S.A.* **95,** 12214 (1998).
91. S. A. Martinis and P. Schimmel, *Proc. Natl. Acad. Sci. U.S.A.* **89,** 65 (1992).
92. S. A. Martinis and P. Schimmel, *J. Biol. Chem.* **268,** 6069 (1993).
93. A. J. Gale and P. Schimmel, *Pharm. Acta Helv.* **71,** 45 (1996).
94. T. Meinnel, Y. Mechulam, S. Blanquet, and G. Fayat, *J. Mol. Biol.* **220,** 205 (1991).
95. M. Frugier, C. Florentz, and R. Giegé, *Proc. Natl. Acad. Sci. U.S.A.* **89,** 3990 (1992).

96. A. R. Fersht and C. Dingwall, *Biochemistry* **18,** 1250 (1979).
97. A. R. Fersht, "Enzyme Structure and Mechanism." W. H. Freeman, New York, 1985.
98. R. B. Loftfield and D. Vanderjagt, *Biochem. J.* **128,** 1353 (1972).
99. L. Lin, S. P. Hale, and P. Schimmel, *Nature (London)* **384,** 33 (1996).
100. R. M. Starzyk, T. A. Webster, and P. Schimmel, *Science* **237,** 1614 (1987).
101. O. Nureki, D. G. Vassylyev, M. Tateno, A. Shimada, T. Nakama, S. Fukai, M. Konno, T. L. Hendrickson, P. Schimmel, and S. Yokoyama, *Science* **280,** 578 (1998).
102. O. Nureki, D. G. Vassylyev, M. Tateno, A. Shimada, T. Nakama, S. Fukai, M. Konno, T. L. Hendrickson, P. Schimmel, and S. Yokoyama, *Science* **283,** 459 (1999).
103. T. K. Nomanbhoy, T. L. Hendrickson, and P. Schimmel, *Mol. Cell* **4,** 519 (1999).
104. L. F. Silvian, J. Wang, and T. A. Steitz, *Science* **285,** 1074 (1999).
105. S. P. Hale, D. S. Auld, E. Schmidt, and P. Schimmel, *Science* **276,** 1250 (1997).
106. M. A. Farrow, B. E. Nordin, and P. Schimmel, *Biochemistry* **38,** 16898 (1999).
107. B. E. Nordin and P. Schimmel, *J. Biol. Chem.* **274,** 6835 (1999).
108. S. P. Hale and P. Schimmel, *Proc. Natl. Acad. Sci. U.S.A.* **93,** 2755 (1996).
109. A. N. Baldwin and P. Berg, *J. Biol. Chem.* **241,** 839 (1966).
110. F. von der Haar and F. Cramer, *Biochemistry* **15,** 4131 (1976).
111. S. P. Hale and P. Schimmel, *Tetrahedron* **53,** 11985 (1997).
112. D. E. Koshland, Jr., *Proc. Natl. Acad. Sci. U.S.A.* **44,** 98 (1958).
113. D. E. Koshland, Jr., G. Nemethy, and D. Filmer, *Biochemistry* **5,** 365 (1966).
114. A. D. Frankel, *Nat. Struct. Biol.* **6,** 1081 (1999).
115. J. R. Williamson, *Nat. Struct. Biol.* **7,** 834 (2000).
116. A. Yaremchuk, S. Cusack, and M. Tukalo, *EMBO J.* **19,** 4745 (2000).
117. B. Delagoutte, D. Moras, and J. Cavarelli, *EMBO J.* **19,** 5599 (2000).
118. J. Cavarelli, B. Delagoutte, G. Eriani, J. Gangloff, and D. Moras, *EMBO J.* **17,** 5438 (1998).
119. P. Brick and D. M. Blow, *J. Mol. Biol.* **194,** 287 (1987).
120. A. R. Fersht, J. W. Knill-Jones, H. Bedoulle, and G. Winter, *Biochemistry* **27,** 1581 (1988).
121. S. Kim, L. Ribas de Pouplana, and P. Schimmel, *Proc. Natl. Acad. Sci. U.S.A.* **90,** 10046 (1993).
122. S. Kim, L. Ribas de Pouplana, and P. Schimmel, *Biochemistry* **33,** 11040 (1994).
123. U. L. RajBhandary, *J. Bacteriol.* **176,** 547 (1994).
124. E. Schmitt, S. Blanquet, and Y. Mechulam, *EMBO J.* **15,** 4749 (1996).
125. V. Ramesh, C. Mayer, M. R. Dyson, S. Gite, and U. L. RajBhandary, *Proc. Natl. Acad. Sci. U.S.A.* **96,** 875 (1999).
126. E. Schmitt, M. Panvert, S. Blanquet, and Y. Mechulam, *EMBO J.* **17,** 6819 (1998).
127. T. Pape, W. Wintermeyer, and M. Rodnina, *EMBO J.* **18,** 3800 (1999).
128. P. J. Beuning and K. Musier-Forsyth, *Biopolymers* **52,** 1 (1999).
129. P. Schimmel and L. Ribas de Pouplana, *Cell (Cambridge, Mass.)* **81,** 983 (1995).
130. L. Ribas de Pouplana, D. D. Buechter, M. W. Davis, and P. Schimmel, *Protein Sci.* **2,** 2259 (1993).
131. P. Schimmel and T. Ripmaster, *Trends Biochem. Sci.* **20,** 333 (1995).
132. J. G. Arnez and D. Moras, *Trends Biochem. Sci.* **22,** 211 (1997).
133. C. Francklyn, K. Musier-Forsyth, and S. A. Martinis, *RNA* **3,** 954 (1997).
134. G. Ghosh, H. Y. Kim, J. P. Demaret, S. Brunie, and L. H. Schulman, *Biochemistry* **30,** 11767 (1991).